Investigation of the suitability of commercially-available CVD diamond for megavoltage x-ray dosimetry.

S.P. Lansley[a,*], G.T. Betzel[a], F. Baluti[a,b], L. Reinisch[a,1], and J. Meyer[a]
[a] Department of Physics & Astronomy, University of Canterbury, Christchurch, New Zealand
[b] Oncology Service, Christchurch Hospital, Christchurch, New Zealand
[*] Corresponding author. E-mail address: stuart.lansley@canterbury.ac.nz
Telephone: +64 3 364 2987 ext. 7587. Fax: +64 3 364 2469

Abstract

Sandwich-type x-ray detectors were fabricated on commercially-available chemical vapour deposition diamond sourced from three manufacturers: Diamond Materials GmbH, Diamonex, and Element Six. These devices were investigated using Raman spectroscopy and 6 megavolt photons from a clinical linear accelerator. Parameters such as the level of the dark (leakage) and photo- currents, necessary priming dose, linearity of photocurrent with dose rate, and device sensitivity were considered. Device characteristics vary considerably. Devices fabricated using Diamonex material required high priming doses, and displayed high dark currents, low photocurrents (and hence low x-ray sensitivity), and non-linear dose-rate responses. In contrast, devices fabricated from Diamond Materials and Element Six material required lower priming doses, and displayed 'zero' dark currents (beyond the detection limit), higher photocurrents and linear dose-rate responses. In addition, the Element Six devices exhibited less variation in response when irradiated at different angles of incidence.

Keywords
Diamond
Synthetic
Chemical vapor deposition
Electrical properties
Detector
6 MV x-rays

1. Introduction

Radiation detection and dosimetry are important in radiation environments such as hospital x-ray imaging and treatment facilities. Dosimetry can be used during patient exposure to confirm the exposure dose, or during system calibration to assess features such as dose or dose rate, depth–dose curves, and beam profiles [1]. For radiotherapy, the dosimetric data obtained during beam calibration are then used during treatment planning to predict the dose absorbed in the patient, in order to ensure optimal delivery of radiation to the tumour whilst minimising the effect on normal, healthy tissue.

[1] Present address: Department of Physical and Earth Sciences, Jacksonville State University, Jacksonville, Alabama, U.S.A.

For radiotherapy, an ideal dosimeter has the following features: high accuracy – the ability to indicate physical dose correctly; high precision – the reproducibility of results under similar conditions; low detection limit – the lowest dose detectable; measurement range – it should be able to detect radiation over an appropriate dose range; linear dose response – readings should be linearly proportional to the given dose; dose-rate independence – readings should be independent of the dose-rate; energy independence – readings should be independent of the radiation energy; and high spatial resolution – it should allow the measurement of the dose in a very small volume [2].

Diamond has been proposed as a material for the construction of radiation detectors for many years, e.g. [3,4]. For applications in radiotherapy, the tissue–equivalence of diamond is seen as an advantage; the atomic number of carbon ($Z = 6$) is close to that of tissue ($Z \approx 7.4$). Also, with diamond being a solid state material with a high atomic density it should be possible to realise small volume detectors suitable for obtaining measurements with high spatial resolution. Diamond has high radiation hardness, meaning that diamond-based dosimeters should be able to withstand higher cumulative doses before device deterioration. It is expected that the response of diamond x-ray detectors should be fairly independent of the x-ray energy and the dose rate. However, diamond does have its drawbacks, including the need for pre-irradiation of the device (priming) in order to stabilise the device response [5].

The early reports of diamond dosimeters for radiotherapy applications utilised carefully selected natural diamonds, and natural diamond-based detectors for radiotherapy applications are commercially-available [6,7]. The scarcity of suitable high-quality natural diamonds results in low quantities of unique detectors that need to be individually calibrated and hence are expensive. Therefore they are not widely used. Developments in the synthesis of diamond during the last couple of decades have led to both chemical vapour deposition (CVD) diamond [8-12] and high pressure high temperature (HPHT) [13-15] diamond being considered for radiotherapy dosimetry. The use of synthetic diamond should make the fabrication of cheaper diamond-based x-ray detectors possible with more reproducible characteristics, resulting from the possibility of controlling the quality of the diamond during synthesis.

The vast majority of authors working with synthetic diamond report results from diamond synthesised in their own laboratories. In this work we report initial results from x-ray detectors constructed from commercially-available CVD diamond films sourced from three commercial suppliers.

2. Experimental Details

2.1. Material

A selection of commercially-available free-standing diamond films was purchased from three manufacturers: Diamond Materials GmbH, a spin-off company from the Fraunhofer Institute IAF in Freiburg, Germany (hereafter referred to as “Diamond Materials” or “DM”) [16]; Diamonex, a business of Morgan Technical Ceramics, which is a division of the Morgan Crucible Company PLC, based in Allentown, Pennsylvania, USA (hereafter referred to as “Diamonex” or “Dx”) [17]; and Element

Six, based on the Isle of Man, British Isles (hereafter referred to as "Element Six" or "E6") [18,19].

Free-standing tiles with nominal thicknesses of 100, 200, and 400 μm were purchased from Diamond Materials. These tiles were 5 mm by 5 mm in size. They were synthesized using chemical vapour deposition (CVD). They had been polished and were described as being of 'optical quality'; hence they were transparent and colourless.

Polycrystalline free-standing tiles with nominal thicknesses of 100, 200, and 400 μm were purchased from Diamonex. These tiles were 5 mm by 5 mm in size. As they were 'as-grown' polycrystalline tiles with random crystallite orientation, the growth surface exhibited considerable surface roughness. A 400–μm–thick 'matte' tile, which had some polishing of the growth surface, was also purchased. All tiles purchased from Diamonex had a black, opaque appearance.

Single–crystal diamond tiles were purchased from Element Six. Two were nominally undoped ([N] <1 ppm, [B] < 0.05 ppm) tiles synthesized using CVD and one was a type Ib ([N] < 200 ppm, [B] < 0.1 ppm) tile synthesized using the high pressure high temperature (HPHT) method [20]. Of the two undoped CVD tiles, one had been polished on one side (average surface roughness, R_a < 10 nm) and lapped on the other (R_a < 250 nm), whereas the other tile had been polished on both sides (R_a < 30 nm). The type Ib HPHT tile had been polished on one side (R_a < 10 nm) and lapped on the other (R_a < 250 nm). All Element Six tiles were 3 mm by 3 mm by 500 μm thick. The two undoped CVD tiles were transparent and colourless, whereas the type Ib HPHT tile was transparent and yellow.

These tiles, and the devices fabricated on them, may hereafter be described using their thickness for the Diamond Materials (DM) and Diamonex (Dx) tiles, e.g. DM100 for the 100–μm–thick tile from Diamond Materials; the 'matte' Diamonex 400–μm-thick tile is designated 'Dx400m'. Element Six (E6) tiles will be described as single–crystal (SC) polished/lapped (PL), polished both sides (P2), or Type Ib (Ib), as per Element Six descriptions.

2.2. Device Fabrication

A sandwich-type device structure was fabricated by deposition of a silver contact (~200 nm thick) on each side of the diamond tile using thermal evaporation through a shadow mask. Circular contacts of 2–mm–diameter were deposited on the 5–mm by 5–mm tiles (Diamond Materials and Diamonex) and 1–mm–diameter circular contacts were deposited on the Element Six 3–mm by 3–mm tiles. Device parameters are summarised in Table 1.

Table 1. Summary of device parameters.

Material		Thickness	Contact	Volume	Bias	Field
Manufacturer	Type	(μm)	(mm ∅)	(mm^3)	(V)	($V \cdot \mu m^{-1}$)
Diamonex	Dx100	100	2	0.31	250	2.50
	Dx200	200	2	0.63	250	1.25
	Dx400	400	2	1.26	250	0.63
	Dx400m	400	2	1.26	250	0.63
Diamond Materials	DM100	100	2	0.31	250	2.50
	DM200	200	2	0.63	250	1.25
	DM400	400	2	1.26	250	0.63
Element Six	E6SCPL	500	1	0.39	250	0.50
	E6SCP2	500	1	0.39	250	0.50
	E6SCIb	500	1	0.39	250	0.50

Each device was glued to the end of a narrow strip of printed circuit board (PCB) and the silver contacts were electrically connected to copper tracks on either side of the PCB. At the opposite end of the PCB physical and electrical connections were made to a triaxial bulkhead connector. The device and PCB were then housed inside a Perspex enclosure (Fig. 1). The enclosure had a total length of about 200 mm and an internal diameter of about 6 mm. The wall thickness was about 3 mm along most of the cavity length and about 1 mm at the end where the device was situated. The external dimensions were chosen as they are the external dimensions of a Perspex build–up cap used at Christchurch Hospital for thimble-type ionisation chambers. This allowed the packaged diamond devices to be used under the same conditions as ionisation chambers. In most of the packaged devices (except the DM200 and E6SCP2 devices) the cavity around the device was filled with a near-tissue equivalent paraffin-based dental wax from Metrodent [21], in order to eliminate the air ambient from around the device. This was to avoid partial loss of electronic equilibrium at the Perspex cavity surface and hence to minimise fluence perturbations [1].

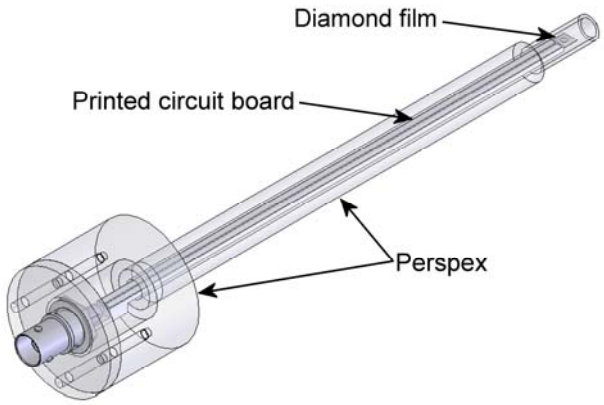

Fig. 1. Schematic of device enclosure.

2.3. Device Characterisation

All x-ray exposure reported in this paper is from exposure to 6 MV photon beams from a Varian 600C treatment linear accelerator in the Oncology Service at Christchurch Hospital, New Zealand. Since the detector is being developed for

radiotherapy applications, the same irradiation geometry and parameters were used as are typically used for beam calibration in radiotherapy.

The device-under-test was inserted into a hole in a stack of blocks of solid water; the external dimensions of the stack were about 30 cm by about 30 cm by 18 cm deep. The device was situated 10 cm deep in the solid water, providing 10 cm of build-up material between the source and the device. The device was positioned at the linear accelerator isocentre giving a source–device distance of 100 cm. A 10×10–cm field size was used for all measurements.

A Farmer 2570/1 dosemeter was used to bias and measure the output of the device. This was placed outside the treatment room and triaxial cabling was used to provide electrical connection between the device and dosemeter, through the treatment room wall. For all results reported in this paper, a constant bias of about 250 V was used, resulting in different electric fields in the devices depending on the thickness of the diamond tile (see Table 1). This dosemeter can only be set to provide a full bias of 250 V or a half, quarter or eighth of this bias, therefore not permitting the same electric field to be used over our range of devices.

The dosemeter was operated manually in the 'Charge'-mode and the output was read out as the charge (nC) measured by the dosemeter over a user-specified time interval, i.e. a time integral of the current through the device. Therefore only an average current during that user-specified time interval could be measured, rather than a true reading of the current through the device. For most results reported here, the charge was measured over a time interval of 4 s, except for the measurements recorded during priming of the devices where a 1–s time interval was used. Within the 'Charge'-mode, the user can select either a 'Low' or 'High' range; the range and resolution of these settings are summarised in Table 2. Using a 4–s integration time, the resolution (and hence detection limit) of the average current is 1.25 pA for the 'Low' range and 12.5 pA for the 'High' range.

Table 2. Range and resolution for the 'Charge'-mode settings on a Farmer 2570/1 dosemeter.

Range switch	Full Scale	Resolution	Maximum continuous input rate
Low	20.475 nC	0.005 nC	6 nA
High	204.75 nC	0.05 nC	60 nA

The gantry angle was kept at 0 degrees for all measurements, i.e. the source being directly overhead. For all measurements except where the angular dependence of the device was measured, the device was held in a horizontal (face-on) orientation such that the x-rays entered the device through the electrical contact to which the bias was applied. During angular dependence measurements the packaged device was rotated within the solid water block (i.e. about the gantry axis of rotation) in order to vary the angle of incidence with respect to the plane of the device, whilst keeping the depth of build-up material constant at 10 cm.

Using the same dosemeter and solid water arrangement, the output of the linear accelerator was assessed by a calibrated thimble-type ionisation chamber (a 0.6 cm^3 Farmer ion chamber). At a depth of 10 cm in the solid water build-up material a dose

of approximately one centigray per monitor unit was measured; the permitted calibration tolerance for clinical application is ±2% from this value. This yields dose rates of approximately 0.5, 1.0, 1.5, 2.0, and 2.5 gray per minute ($Gy \cdot min^{-1}$) for the linear accelerator preset nominal dose rates of 50, 100, 150, 200, and 250 monitor units per minute ($MU \cdot min^{-1}$) respectively.

3. Results & Discussion

3.1. Raman Spectroscopy

Raman spectroscopy with a 514.5–nm argon laser was initially used to investigate the crystalline quality of the diamond films before the electrodes were added to the films (Fig. 2); all spectra were normalised to the intensity of the diamond Raman peak. The first-order diamond Raman peak at 1332 wavenumbers is clearly evident in all samples. No other noticeable peaks which could be attributable to non-diamond carbon phases are observed in the range 1200–1600 wavenumbers, indicating good quality, clean diamond. The peak at 2050 wavenumbers (575 nm) observed in most spectra and the broad background photoluminescence (particularly noticeable in the Diamonex material, Fig. 2(a, b)) are both due to nitrogen–vacancy (NV) complexes in the diamond crystal [22]. The intensity of the 2050–wavenumber peak (relative to the diamond Raman peak) and the background photoluminescence were much higher for the polycrystalline Diamonex material (Fig. 2(a, b)) than they were for the Diamond Materials or Element Six material (Fig. 2(c-h)).

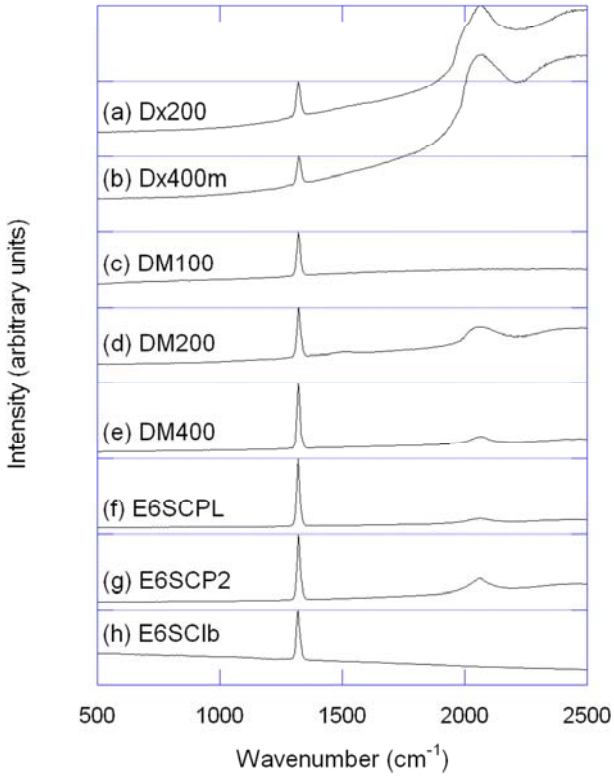

Fig. 2. Raman spectra of (a) Dx200, (b) Dx400m, (c) DM100, (d) DM200, (e) DM400, (f) E6SCPL, (g) E6SCP2, and (h) E6SCIb; all spectra were normalised to the intensity of the diamond Raman peak. 514.5–nm Ar laser excitation was used.

The spectrum of the yellow HPHT type Ib (nitrogen-containing) diamond does not display these features (Fig. 2 (h)). Yellow diamonds obtain their colour from the N3 system, which appears as several luminescence peaks in the 400–500 nm range and hence is too short to be observed with the 514.5–nm laser used during these experiments.

3.2. Initial/Un-primed Response

The initial responses of the fabricated devices to exposure to an x-ray beam of dose rate 250 MU·min^{-1} are shown in Fig. 3; horizontal error bars indicate the 4-s intervals during which the average current was measured, and vertical error bars indicate uncertainties in the average current, arising from the resolution of the Farmer dosemeter. The beam was turned on at 17 seconds (after three readings with the beam off) and off at 53 seconds (after six readings with the beam on), as indicated in Fig. 3(a). Different responses were observed from the devices fabricated on material from the three suppliers.

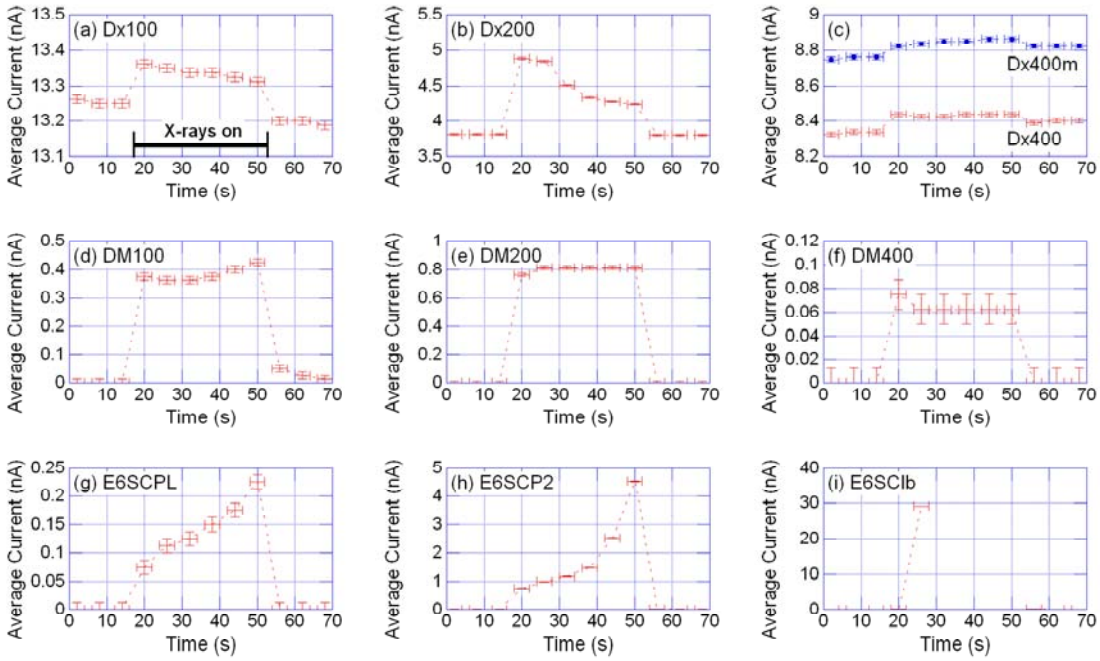

Fig. 3. Initial (un-primed) response of devices fabricated on (a-c) Diamonex, (d-f) Diamond Materials, and (g-i) Element Six synthetic diamond. In each case, a 250–MU·min^{-1} x-ray beam was turned on at 17 seconds and off at 53 seconds, as indicated in (a).

Devices fabricated on material from Diamonex (Fig. 3(a-c)) exhibited dark currents of the order of several nA. An increase in the current through the devices was observed when the devices were exposed to the x-rays. The change in current ranged from less than one percent for Dx100, Dx400 and Dx400m, to a 'steady-state' value of about ten percent with an initial transient of over 25% for Dx200. The dark current was observed to change with time and/or exposure to the x-rays. For the 100– and 200–µm devices the dark current reduced with time and/or x-ray exposure, whereas an increase in dark current was observed for the 400–µm–thick devices. This combination of characteristics – a high, varying dark current, combined with a

relatively small photocurrent – does not initially indicate potential for use as a sensitive, accurate x-ray detector with an easily-measureable response.

Devices fabricated on the Diamond Materials and Element Six material all exhibited 'zero' dark current, below the detection limit of the Farmer 2570/1 dosemeter. However, device DM100 showed some persistent photocurrent when the x-ray beam was switched off (Fig. 3(d)), indicating that this device may be slow to 'turn off'.

Devices DM200 and DM400 appeared to have reached a steady-state of conduction during the time of exposure to the x-rays, whereas the current in device DM100 had not reached a steady-state and was still increasing prior to the x-ray beam being switched off. A (photo-)current increasing with time, and hence dose, is also observed in the devices fabricated from Element Six material. This is likely to imply that these devices have slow response times, some priming mechanism is taking place, or some combination of these two effects is being observed. The turn-off of these devices (i.e. those fabricated on Diamond Materials and Element Six material) is fairly quick, as the average current measured in these devices (excluding DM100) is less than 1.25 pA when measured over 4 seconds soon after x-ray exposure is ceased. Hence priming appears to be the main reason for the increasing currents observed during x-ray exposure of the E6SCPL and E6SCP2 devices. A combination of slow response time and priming may have been observed for device DM100, due to the exponential decay-like reduction of the current observed after ceasing exposure to the x-rays. In the case of device E6SCIb, the conductivity of the device increased to such an extent that the maximum continuous input rate of the Farmer 2570/1 dosemeter (60 nA on the 'High' range – see Table 2) was exceeded during the 4–s integration time after only two readings could be taken during x-ray exposure. A shorter integration time could not be used, as the current through the device would still have exceeded this limit. This limit was also exceeded when the dose rate was reduced to the lowest setting available (50 $MU \cdot min^{-1}$ rather than 250 $MU \cdot min^{-1}$). Therefore it was not possible to obtain any meaningful data from this device.

3.3. Priming

During priming of the devices fabricated from Diamond Materials and Element Six material the devices were exposed to the x-rays using a dose rate of 250 $MU \cdot min^{-1}$ (~2.5 $Gy \cdot min^{-1}$). As these devices showed 'zero' dark current it was straightforward to measure the current during the priming in order to assess the effect that the priming had on the device response, i.e. the photocurrent. This effect can be seen in Fig. 4; error bars are not shown as the uncertainties are small relative to the measured values.

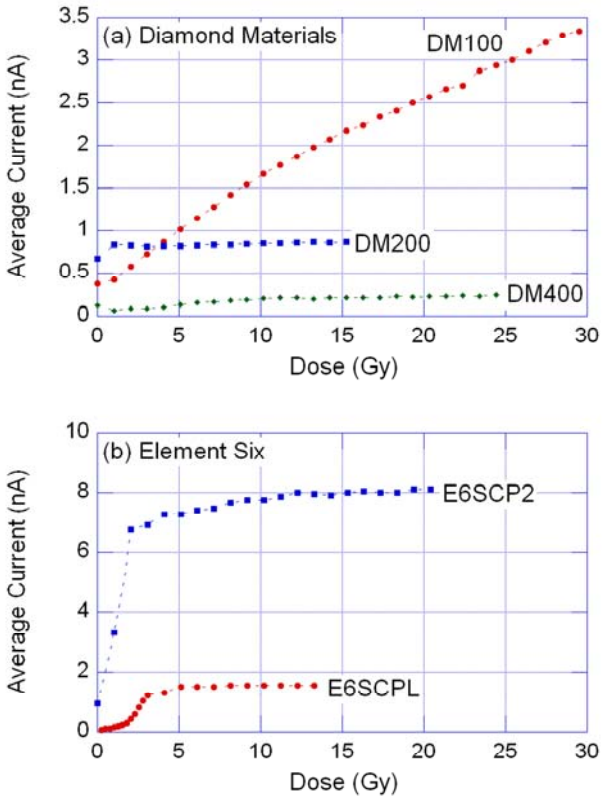

Fig. 4. The effect of priming on the response of devices fabricated on material obtained from (a) Diamond Materials and (b) Element Six. A dose rate of 250 $MU \cdot min^{-1}$ (~2.5 $Gy \cdot min^{-1}$) was used.

Devices DM200 and DM400 showed a small change in response at low doses (<10 gray) but then appeared to be quite stable (Fig. 4(a)). These two devices appear to need only a small priming dose. Device DM100, however, showed a response that continued to be increasing after about 30 Gy of irradiation.

The two devices fabricated on Element Six undoped single–crystal CVD diamond (E6SCPL and E6SCP2) also required low priming doses before their responses appeared to plateau (Fig. 4(b)), reaching levels of about 1.6 nA for E6SCPL and about 8 nA for E6SCP2.

The non-zero dark current observed in the Diamonex devices meant that both the dark current and light current (i.e. total of dark current and photocurrent during x-ray irradiation) needed to be considered during investigation of the priming of these devices. The evolution of these currents for device Dx200 is shown in Fig. 5; error bars are not shown as the uncertainties are about 40 mGy in the dose and 1.25 pA in the current. The device was irradiated with a dose rate of 250 $MU \cdot min^{-1}$ (~2.5 $Gy \cdot min^{-1}$) to yield the 'X-rays ON' data, and the x-ray beam was repeatedly switched off and on in order to measure the dark current ('X-rays OFF' data). Exponential-decay curve fits through the data sets were used to show the trends. The dark current appears to be tending towards ~3.5 nA with a decay constant of ~55 Gy, and the light current towards ~6.3 nA with a decay constant of ~23 Gy.

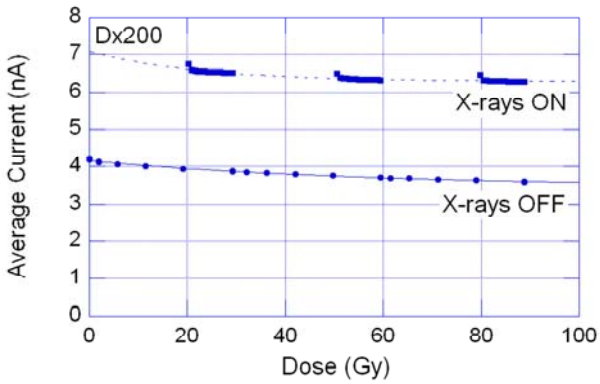

Fig. 5. The effect of priming on the response of device Dx200, showing dark current ('X-rays OFF') and light current ('X-rays ON'); an exponential decay fit is plotted for each set of data as a trend line.

Usually, an increase in current is observed during priming, as seen for the Diamond Materials and Element Six devices shown in Fig. 4. This was not observed for the Diamonex devices (e.g. Fig. 5). However, a slight reduction in photocurrent (the difference in current between when the x-ray beam is on and when it is off) was observed between 0 and about 40 Gy, followed by a slight increase from 40 Gy, appearing to reach a steady-state after a dose of about 300 Gy (data not shown). It is not obvious why this different effect was observed for devices fabricated from Diamonex material. It may arise from the grain boundaries in this polycrystalline material. Regardless of the origin of this effect, it is obvious that, due to this unfavourable characteristic, this material is not well-suited to this application.

The minimum priming dose for each device was estimated from Fig. 4 and Fig. 5. These values are summarised in Table 3, along with the minimum priming dose per micrometre thickness for each device; these data are intended to provide relative magnitudes rather than exact values. For devices Dx200 and DM100, full priming did not occur over the dose shown in the corresponding figures, and hence the minimum priming doses have been estimated from extrapolated curve fits.

Table 3. Summary of device performance.

Material		Min. Priming Dose		Power Law Fit ($I_{ph} = k\dot{D}^{\Delta}$)		Approx. Linear Sensitivity	
Manufacturer	Type	(Gy)	(Gy·μm^{-1})	k	Δ	(nC·Gy^{-1})	(nC·Gy^{-1}·mm^{-3})
Diamonex	Dx100	>100 (~300[a])	>1 (~3[a])	2.00e-4 ± 5.3e-5	1.16 ± 0.05	3.14	10.0
	Dx200	>100 (~300[a])	>0.5 (~1.5[a])	6.55e-3 ± 6.4e-4	0.61 ± 0.02	3.54	5.64
	Dx400	-	-	-	-	-	-
	Dx400m	-	-	-	-	-	-
Diamond Materials	DM100	>>30 (~200[a])	>>0.3 (~2[a])	-	-	-	-
	DM200	~1	~0.005	5.04e-3 ± 5.0e-4	0.94 ± 0.02	20.2	32.2
	DM400	~10	~0.025	1.00e-3 ± 5e-5	1.00 ± 0.01	5.94	4.72
Element Six	E6SCPL	~5	~0.01	6.25e-3 ± 3.0e-4	1.00 ± 0.01	37.0	94.3
	E6SCP2	~10	~0.02	2.82e-2 ± 8e-4	1.01 ± 0.01	178	454
	E6SCIb	-	-	-	-	-	-

[a] Estimated from extrapolated curve fit.

3.4. Primed Response

The response of 'primed' devices on material from all three suppliers is shown in Fig. 6; horizontal error bars indicate the 4-s intervals during which the average current was measured. Vertical error bars are not shown; the uncertainty in the current is 12.5 pA for the Diamonex devices and E6SCP2, and 1.25 pA for Diamond Materials devices and E6SCPL. The measurements consisted of alternating periods with and without exposure to the x-ray beam, and with increasing dose rates, as shown by the text at the top of the figure.

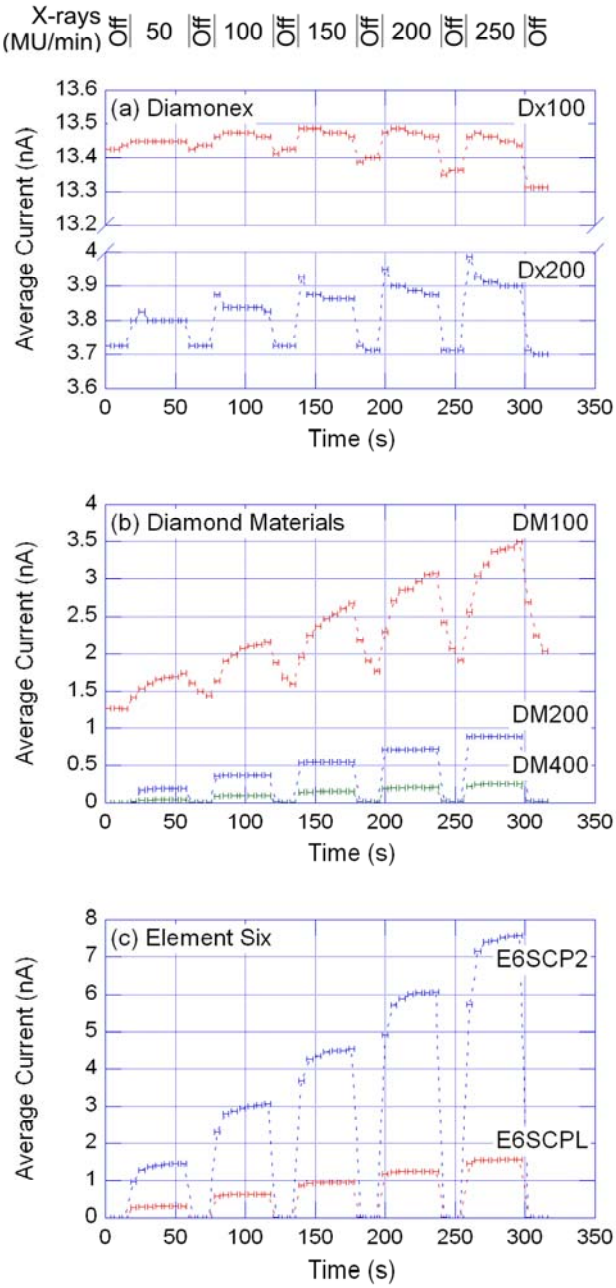

Fig. 6. After priming responses of (a) Diamonex, (b) Diamond Materials, and (c) Element Six devices to dose rates of 50, 100, 150, 200, and 250 MU·min^{-1}, as indicated at the top of the figure.

A small change in current was observed when the Diamonex devices were exposed to the x-ray beam (Fig. 6(a)). The dark current through these devices continued to reduce with continuing exposure to the radiation. A brief overshoot was seen with the device Dx200 when the x-ray beam was turned on.

Diamond Materials devices DM200 and DM400 continued to exhibit 'zero' dark current and a step-like change in current when they were irradiated with the x-rays (Fig. 6(b)). Device DM100, however, continued to display slow rise and fall times (Fig. 6(b)).

As with the Diamond Materials devices, the Element Six devices retained their 'zero' dark current (Fig. 6(c)). They also responded in a step-like fashion to the increasing x-ray dose rates, but with a slower rise time than that seen for the Diamond Materials devices.

The steady-state photocurrent (i.e. the steady-state of the current after subtraction of the background dark current) is shown as a function of the dose rate in Fig. 7. A power-law relationship between the photoconductivity (σ) and the dose rate ($\dot{D}$) is expected according to [23] where the exponent (Δ) usually lies between 0.5 and 1.0. If there are no traps or when the excitation rate is so high that traps are unimportant, $\Delta = 0.5$ while uniform or quasi-uniform trap distributions over a range of depths in the forbidden energy gap should lead to $\Delta \approx 1$ [23]. Photocurrent (I_{ph}) is proportional to photoconductivity, and hence power law curve fits to the data are shown in Fig. 7. The multiplier (k) and exponent (Δ) values are summarised in Table 3.

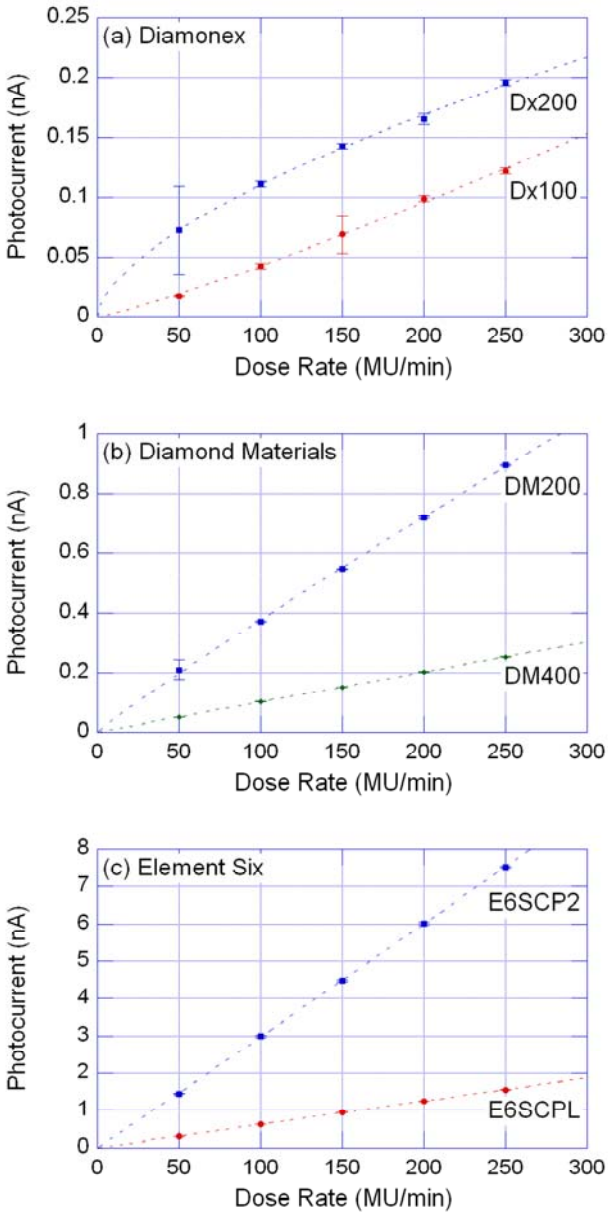

Fig. 7. Steady-state photocurrent as a function of dose rate; 100 MU·min^{-1} is ~1 Gy·min^{-1}. Power-law curve fits are shown for all devices.

For all devices shown in Fig. 7, a power-law curve suitably describes the data; R^2 values for the curve fits are greater than 0.997 for the Diamonex devices and 0.999 for the Diamond Materials and Element Six devices. The exponent (Δ) values appear to vary from 0.61 for Dx200 to 1.16 for Dx100. Three devices — DM400 and the two Element Six devices — have exponents close to unity, indicating uniform or quasi-uniform trap distributions [23]; a unity power-law exponent is a highly desirable characteristic of a detector, as it indicates that the photocurrent is linearly-dependent on the dose rate (whilst passing through the origin), thus simplifying calculation of the dose rate from the photocurrent. The sensitivity of these three devices was measured at about 6, 37, and 178 nC·Gy^{-1} for DM400, E6SCPL and E6SCP2, respectively.

Observing the data for the other three devices (Dx100, Dx200, and DM200), it would not be unreasonable to consider using a linear fit through the data points, although such curve fits would not pass through the origin. Over the dose rate range used here (50—250 MU·min^{-1}), the sensitivity of these devices are about 3, 3.5, and 20 nC·Gy^{-1}, respectively; R^2 values of greater than 0.998 were measured for linear fits to these three sets of data.

Exponent values reported in the literature lie in the range 0.92–1 for PTW diamond detectors [24-29], 0.86–1.035 for CVD diamond [24,25,30-32], and 0.49–0.97 for HPHT diamond [13,14]. The values observed for the devices fabricated on Diamond Materials and Element Six diamond films are close to one and hence compare well to the literature. However, the Diamonex devices do not, which may be due to errors in the measurement of the photocurrent, arising from low photocurrent levels and significant, decreasing dark current levels.

The specific sensitivity is the device sensitivity divided by the device volume. Assuming the device volume to be the contact area multiplied by the manufacturer's quoted film thickness, this yields specific sensitivities of about 10, 6, 32, 5, 94, and 454 nC·Gy^{-1}·mm^{-3} for devices Dx100, Dx200, DM200, DM400, E6SCPL, and E6SCP2, respectively, as listed in Table 3; these values were obtained with applied electric fields of about 2.50, 1.25, 1.25, 0.63, 0.50, and 0.50 V·μm^{-1} for devices Dx100, Dx200, DM200, DM400, E6SCPL, and E6SCP2, respectively, as listed in Table 1.

Specific sensitivities values reported in the literature have been measured using a variety of x-ray (250 kV, and 6, 10, and 25 MV) and electron (4–25 MeV) energies from linear accelerators, as well as other radiation sources such as ^{60}Co and ^{90}Sr. For PTW natural diamond detectors the specific sensitivities lie in the range 50–140 nC·Gy^{-1}·mm^{-3} [8,24,26,27,33]. A wide range of specific sensitivities have been reported for CVD diamond-based detectors, ranging from a few to over a thousand nC·Gy^{-1}·mm^{-3}; generally, the lower values (of up to ~100 nC·Gy^{-1}·mm^{-3}) appear to be reported for polycrystalline material grown in-house by the researchers [8,9,25,30,34], whereas the higher values were obtained using commercial CVD diamond, some of which was described as 'detector grade' [10,24,31,34,35]. Values between 18 and 164 nC·Gy^{-1}·mm^{-3} have been reported for detectors based on HPHT diamonds [14]. For comparison, Bruzzi *et al.* reported the following typical values for standard on-

line dosimeters: standard 0.6 cm^3 Farmer ionisation chamber, 0.036 $nC \cdot Gy^{-1} \cdot mm^{-3}$; miniature EXRADIN T1 ionisation chamber, 0.028 $nC \cdot Gy^{-1} \cdot mm^{-3}$; Scanditronix GR-p BS silicon diode, 474 $nC \cdot Gy^{-1} \cdot mm^{-3}$; and Scanditronix SFD stereotactic diode, 353 $nC \cdot Gy^{-1} \cdot mm^{-3}$ [36]. Other values reported include 330 $nC \cdot Gy^{-1} \cdot mm^{-3}$ for an epitaxial SiC diode [36] and 128–480 $nC \cdot Gy^{-1} \cdot mm^{-3}$ for polymer-based detectors [37].

The specific sensitivities reported here for devices fabricated using Diamonex and Diamond Materials diamond are comparable to the values reported for in-house grown CVD diamond, whereas the values obtained from our Element Six diamond-based devices are comparable to other values reported from high-quality commercial diamond.

The measured sensitivity and specific sensitivity values depend on the device geometry (contact area and film thickness). They will also depend on the voltage and hence electric field applied. The Element Six material was thicker than the other material (500 μm compared to 100, 200, or 400 μm) and the fabricated devices consisted of smaller contact area than the other devices (1 mm diameter contacts compared to 2 mm diameter); see Table 1. A larger contact area should result in a larger current through the device, as the resistance is inversely proportional to the area. The thickness of the diamond would affect the device performance in at least two ways: the thicker the material, the greater the distance over which the x-rays can interact with the material, resulting in a greater number of mobile charge carriers and hence an increase in current; however, if a constant bias were used for all devices, a smaller electric field would be present in the thicker devices resulting in smaller currents than if the same field had been applied to all devices – resistance being proportional to thickness. Therefore, doubling the contact area and halving the device thickness will not change the device volume but is likely to reduce the resistance of the device (through both the increase in area and the decrease in thickness) and therefore is likely to result in increased sensitivity and specific sensitivity.

The device response was also investigated as a function of the angle of irradiation (Fig. 8). Face-on irradiation occurs for incident angles of 0° and 180°, with 0° corresponding to irradiation through the positively biased contact. Edge-on irradiation occurs for incident angles of 90° and 270°. For these data, the steady-state current was measured using a dose rate of 250 $MU \cdot min^{-1}$ (~2.5 $Gy \cdot min^{-1}$) and the data for each device were normalised using the maximum photocurrent obtained for that device. The results were recorded with increasing angle of irradiation.

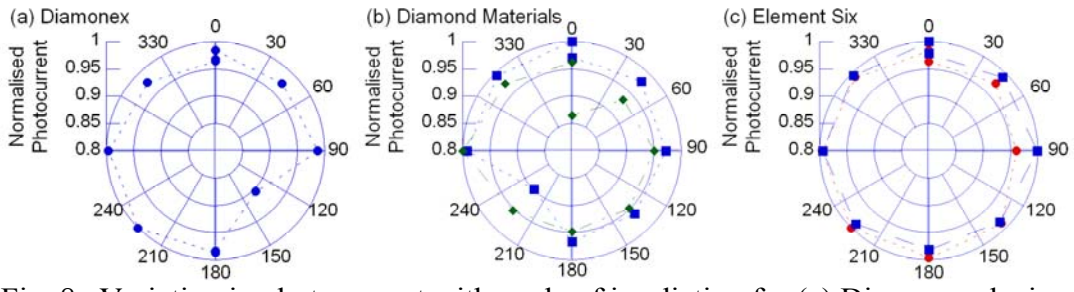

Fig. 8. Variation in photocurrent with angle of irradiation for (a) Diamonex device Dx200, (b) Diamond Materials devices DM200 (■) and DM400 (♦), and (c) Element Six devices E6SCPL (●) and E6SCP2 (■). 0° is perpendicular to the film with irradiation through the positive contact. A dose rate of 250 $MU \cdot min^{-1}$ was used.

A small angular dependence was seen. The photocurrent was observed to vary by less than ten percent during these measurements, with the smallest variation (less than five percent) observed for the Element Six material, in particular material E6SCPL (about two percent). However, there appeared to be either a slight increase or decrease of the photocurrent during the measurements, as the initial and final 0° measurements did not line up. The photoresponse of Diamonex device Dx200 appeared to have reduced slightly during the measurements, whereas an increase in photoresponse was seen for the Diamond Materials and Element Six devices. These trends are in the same direction as observed during priming; therefore they may be explained by the priming characteristics of these devices if priming was continuing during these measurements.

4. Conclusions

Sandwich-configuration device structures were fabricated on commercially-available material from three manufacturers (Diamond Materials GmbH, Diamonex, and Element Six) in order to assess the material for use in megavoltage x-ray dosimetry for radiotherapy applications.

Diamonex material does not appear to be particularly suited for such applications. Devices fabricated from this material exhibited significant, and varying, dark currents, which are not desirable as this means that each reading requires measurement of the current both with the x-ray beam on and with the x-ray beam off, thereby complicating the measurement procedure. Low sensitivity (a few $nC \cdot Gy^{-1}$) arises from the low photocurrent generated during x-ray exposure. A linear relationship between dose rate and photocurrent is desirable, but a non-linear relationship was observed for both Dx100 ($\Delta = 1.16$) and Dx200 ($\Delta = 0.61$).

Diamond Materials GmbH material appears more suitable for use as a x-ray detector material because of the following characteristics: very low dark currents (below the dosemeter detection limit), making measurement of the photocurrent simple; the low priming dose needed (<10 Gy); linear relationship between dose rate and photocurrent; higher sensitivity; and reasonable turn-on and turn-off times, although the speed of response was not specifically investigated as the experimental set-up (in particular the dosemeter) was not suitable to do this. However, the particular piece of material DM100 tested did not display these desirable characteristics and therefore does not appear to be particularly suitable for this application. It did not appear to be fully primed after a dose of 30 Gy, having not reached a steady-state. Also, it exhibited slower turn-on and turn-off times, yielding light and dark currents which did not reach steady-state values during the time scale used. This would make it difficult to determine the photocurrent, and hence the dose rate dependence.

The undoped material from Element Six displayed the following characteristics, which appear to make it a suitable candidate for the fabrication of x-ray detectors: very low dark current (as with the Diamond Materials films, this was below the detection limit of the dosemeter used during characterisation); a low dose (~10 Gy) was needed to prime the devices; response times that are acceptable on the current time scale; linear dose rate response; good sensitivity; and the smallest angular variation.

Raman spectra obtained from the diamond films all clearly showed the diamond first-order Raman peak. Most of the films also showed a peak at about 2050 wavenumbers and a broad photoluminescence background, both of which are attributable to NV complexes. In the spectra of the Diamonex films, the signals from these features were more intense than those from the diamond first-order Raman peak; these films are not particularly suited to dosimetry applications. The four films which displayed good dosimeter characteristics (DM200, DM400, E6SCPL, and E6SCP2) also exhibited these NV features but at lower intensities than the diamond first-order Raman peak. Two films (DM100 and E6SCIb) did not display the NV features. Detectors fabricated on these films were not suited to the experimental arrangement used during these measurements; DM100 required a priming dose greater than it received during these experiments as it had not reached a stable plateau after an exposure of 30 Gy and also it was slow to turn on and off, whereas E6SCIb became too conductive for the Farmer dosemeter to measure.

All devices except DM200 and E6SCP2 had the cavity around the device filled with dental wax to eliminate the air void around the device. No notable differences in the device characteristics are immediately attributable to the presence or absence of the wax. A higher sensitivity was observed in DM200 (without wax) than in DM400 (with wax), but this may be due to the higher applied field; the same bias was applied across a thinner film. E6SCP2 (without wax) was also more sensitive than E6SCPL (with wax), but this may be as a result of the surface polishing. Further experiments into the effect of filling the cavity with wax are on-going.

Devices fabricated from Element Six material warrant further examination, to investigate device characteristics such as stability, repeatability, depth–dose curves and off-axis profiles.

Acknowledgements

The authors would like to acknowledge Joon Koo (Scott) Choi from the Department of Physics & Astronomy at the University of Canterbury for his assistance with the Raman spectroscopy measurements.

S.P. Lansley would like to acknowledge the Foundation for Research, Science and Technology (FRST), New Zealand, for the receipt of a NZ Science and Technology Post-doctoral Fellowship (UOCX0702).

G.T. Betzel was funded in part by Sigma Xi Grants-in-Aid of Research.

References

[1] F.M. Khan, The Physics of Radiation Therapy, 3rd ed., Lippincott Williams & Wilkins, Philadelphia, 2003.
[2] P. Metcalfe, T. Kron, P. Hoban, The Physics of Radiotherapy X-Rays from Linear Accelerators, Medical Physics Pub, Madison, Wis, 1997.
[3] B. Planskoy, Physics in Medicine and Biology 25 (1980) 519-532.
[4] E. Burgemeister, Physics in Medicine and Biology 26 (1981) 269-275.
[5] P. Bergonzo, D. Tromson, C. Descamps, H. Hamrita, C. Mer, N. Tranchant, M. Nesladek, Diamond and Related Materials 16 (2007) 1038-1043.

[6] V. Khrunov, S. Martynov, S. Vatnitsky, I. Ermakov, A. Chervjakov, D. Karlin, V. Fominych, Y. V. Tarbeyev, Radiat Prot Dosimetry 33 (1990) 155-157.
[7] PTW Diamond Detector, http://www.ptw.de/diamond_detector0.html?&L=0
[8] A. Fidanzio, L. Azario, C. Venanzi, F. Pinzari, A. Piermattei, Nuclear Instruments and Methods in Physics Research Section A: Accelerators, Spectrometers, Detectors and Associated Equipment 479 (2002) 661-667.
[9] C.M. Buttar, J. Conway, R. Meyfarth, G. Scarsbrook, P.J. Sellin, A. Whitehead, Nuclear Instruments and Methods in Physics Research Section A: Accelerators, Spectrometers, Detectors and Associated Equipment 392 (1997) 281-284.
[10] M. Bruzzi, M. Bucciolini, G. Cirrone, G. Cuttone, A. Guasti, S. Mazzocchi, S. Pirollo, M. Sabini, S. Sciortino, Nuclear Science, IEEE Transactions On 47 (2000) 1430-1433.
[11] G. Cuttone, L. Azario, L. Barone Tonghi, E. Borchi, D. Boscarino, M. Bruzzi, M. Bucciolini, G.A.P. Cirrone, C. De Angelis, G. Della Mea, P. Fattibene, C. Gori, A. Guasti, S. Maggioni, S. Mazzocchi, S. Onori, M. Pacilio, E. Petetti, A. Piermattei, S. Pirollo, A. Quaranta, L. Raffaele, V. Rigato, A. Rovelli, M.G. Sabini, S. Sciortino, G. Zatelli, Nuclear Physics B - Proceedings Supplements 78 (1999) 587-591.
[12] P. Bergonzo, D. Tromson, C. Mer, Semiconductor Science and Technology 18 (2003) S105-S112.
[13] B. Marczewska, T. Nowak, P. Olko, W. Gajewski, Y. Pal'yanov, I. Kupriyanov, M. Waligorski, Diamond and Related Materials 13 (2004) 918-922.
[14] B. Marczewska, I. Kupriyanov, Y. Pal'yanov, T. Nowak, P. Olko, M. Rebisz, M. Waligorski, Diamond and Related Materials 16 (2007) 191-195.
[15] F. Schirru, I. Kupriyanov, B. Marczewska, T. Nowak, Physica Status Solidi (a) 205 (2008) 2216-2220.
[16] Diamond Materials: Advanced Diamond Technology, http://www.diamond-materials.de/index_en.html
[17] Diamonex - A Leasding Supplier of DLC Coatings and CVD Diamond Products, http://www.diamonex.com
[18] Element Six - Home, http://www.e6.com/en/
[19] Synthetic CVD Diamond Products from Element Six, http://www.e6cvd.com
[20] Single Crystal Diamond Plate, http://193.120.252.126/cvd/page.jsp?pageid=1003
[21] Metrodent, http://www.metrodent.com
[22] C. Descamps, D. Tromson, C. Mer, M. Nesladek, P. Bergonzo, M. Benabdesselam, Physica Status Solidi (a) 203 (2006) 3161-3166.
[23] J. Fowler, in:, Radiation Dosimetry, Academic, New York, 1966.
[24] M. Bucciolini, E. Borchi, M. Bruzzi, M. Casati, P. Cirrone, G. Cuttone, C. De Angelis, I. Lovik, S. Onori, L. Raffaele, S. Sciortino, Nuclear Instruments and Methods in Physics Research Section A: Accelerators, Spectrometers, Detectors and Associated Equipment 552 (2005) 189-196.
[25] A. Fidanzio, L. Azario, P. Viola, P. Ascarelli, E. Cappelli, G. Conte, A. Piermattei, Nuclear Instruments and Methods in Physics Research Section A: Accelerators, Spectrometers, Detectors and Associated Equipment 524 (2004) 115-123.
[26] P.W. Hoban, M. Heydarian, W.A. Beckham, A.H. Beddoe, Physics in Medicine and Biology 29 (1994) 1219-1229.
[27] W.U. Laub, T.W. Kaulich, F. Nusslin, Med. Phys. 24 (1997) 535-536.
[28] W.U. Laub, T.W. Kaulich, F. Nusslin, Physics in Medicine and Biology 44 (1999) 2183-2192.

[29] S.N. Rustgi, D.M.D. Frye, Med. Phys. 22 (1995) 2117-2121.
[30] B. Górka, B. Nilsson, R. Svensson, A. Brahme, P. Ascarelli, D. Trucchi, G. Conte, R. Kalish, Physica Medica 24 (2008) 159-168.
[31] G. Cirrone, G. Cuttone, S. Lo Nigro, V. Mongelli, L. Raffaele, M. Sabini, Nuclear Physics B - Proceedings Supplements 150 (2006) 330-333.
[32] C.M. Buttar, R. Airey, J. Conway, G. Hill, S. Ramkumar, G. Scarsbrook, R.S. Sussmann, S. Walker, A. Whitehead, Diamond and Related Materials 9 (2000) 965-969.
[33] M. Heydarian, P.W. Hoban, W.A. Beckham, I.M. Borchardt, A.H. Beddoe, Physics in Medicine and Biology 38 (1993) 1035-1042.
[34] M. Bruzzi, M. Bucciolini, G.A.P. Cirrone, G. Cuttone, S. Mazzocchi, S. Pirollo, S. Sciortino, Nuclear Instruments and Methods in Physics Research Section A: Accelerators, Spectrometers, Detectors and Associated Equipment 454 (2000) 142-146.
[35] M. Bruzzi, M. Bucciolini, M. Casati, C. DeAngelis, S. Lagomarsino, I. Lovik, S. Onori, S. Sciortino, Nuclear Instruments and Methods in Physics Research Section A: Accelerators, Spectrometers, Detectors and Associated Equipment 518 (2004) 421-422.
[36] M. Bruzzi, M. Bucciolini, F. Nava, S. Pini, S. Russo, Nuclear Instruments and Methods in Physics Research Section A: Accelerators, Spectrometers, Detectors and Associated Equipment 485 (2002) 172-177.
[37] F.A. Boroumand, M. Zhu, A.B. Dalton, J.L. Keddie, P.J. Sellin, J.J. Gutierrez, Appl. Phys. Lett. 91 (2007) 033509-3.

Erratum

Erratum to "Investigation of the suitability of commercially available CVD diamond for megavoltage X-ray dosimetry"

[Nucl. Instr. and Meth. A 607 (2009) 659–667]

S.P. Lansley[a,*], G.T. Betzel[a], F. Baluti[a,b], L. Reinisch[a,1], J. Meyer[a]
[a] Department of Physics and Astronomy, University of Canterbury, Christchurch, New Zealand
[b] Oncology Service, Christchurch Hospital, Christchurch, New Zealand

Available online 17 June 2009

An incorrect conversion from monitor units (MU) to gray (Gy) was used for the doses and dose rates our devices were exposed to. The quoted conversion factor of approximately 1 centigray (cGy)/monitor unit actually refers to measurements at the isocentre but with 1.5 cm build-up material. Therefore, the values should have been multiplied by the appropriate Tissue Maximum Ratio (TMR) for the linear accelerator used (0.778) in order to obtain the doses and dose rates at the isocentre with 10 cm solid water build-up material. Thus, in the original article, doses and dose rates (where quoted in gray) were over-stated. As a result of this, the sensitivities of our devices were under-stated.

This conversion affected Figures 4 and 5, Table 3, and dose and dose rate values where quoted in gray in the text. The correct versions of Figures 4 and 5, and Table 3 can be found below.

The authors would like to thank Mark Bird (Oncology Service, Christchurch Hospital) for his help in checking this correction.

Table 3. Summary of device performance.

Material		Min. Priming Dose		Power Law Fit ($I_{ph} = k\dot{D}^{\Delta}$)		Approx. Linear Sensitivity	
Manufacturer	Type	(Gy)	(Gy μm^{-1})	k	Δ	(nC Gy^{-1})	(nC Gy^{-1} mm^{-3})
Diamonex	Dx100	>70 (~230[a])	>0.7 (~2.3[a])	2.00e-4 ± 5.3e-5	1.16 ± 0.05	4.08	13.0
	Dx200	>70 (~230[a])	>0.35 (~1.15[a])	6.55e-3 ± 6.4e-4	0.61 ± 0.02	4.61	7.34
	Dx400	-	-	-	-	-	-
	Dx400m	-	-	-	-	-	-
Diamond Materials	DM100	>>25 (~150[a])	>>0.25 (~1.5[a])	-	-	-	-
	DM200	<1	<0.005	5.04e-3 ± 5.0e-4	0.94 ± 0.02	26.1	41.5
	DM400	<10	<0.025	1.00e-3 ± 5e-5	1.00 ± 0.01	7.65	6.09
Element Six	E6SCPL	<5	<0.01	6.25e-3 ± 3.0e-4	1.00 ± 0.01	47.7	121
	E6SCP2	<10	<0.02	2.82e-2 ± 8e-4	1.01 ± 0.01	230	586
	E6SCIb	-	-	-	-	-	-

[a] Estimated from extrapolated curve fit.

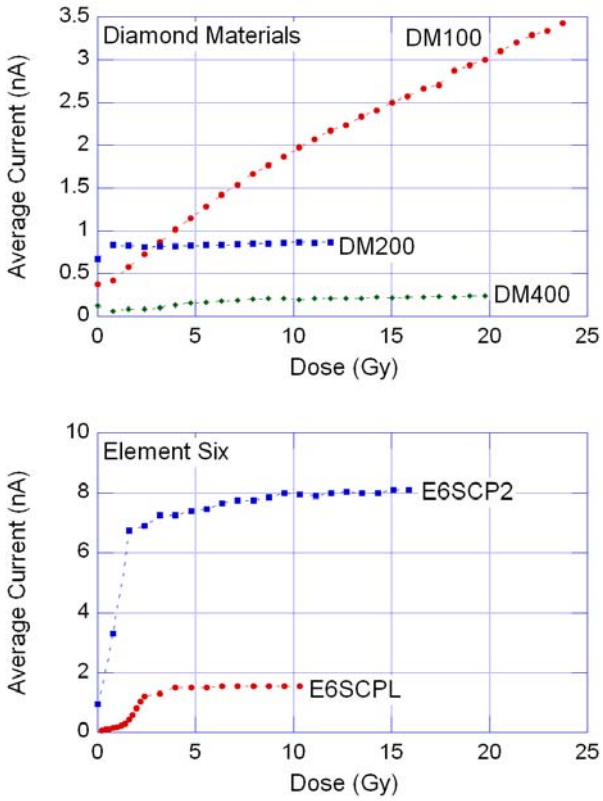

Fig. 4. Effect of priming on the response of devices fabricated on material obtained from (a) Diamond Materials and (b) Element Six. A dose rate of 250 MU min^{-1} (~1.9 Gy min^{-1}) was used.

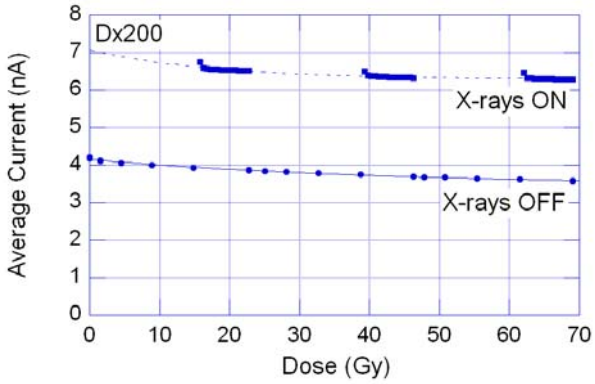

Fig. 5. Effect of priming on the response of device Dx200, showing dark current ('X-rays OFF') and light current ('X-rays ON'); an exponential-decay fit is plotted for each set of data as a trend line.